PNAS
www.pnas.org

Supplementary Information for

Histone 2B monoubiquitination complex integrates transcript elongation with splicing at circadian clock and flowering time regulators

Magdalena Woloszynska, Sabine Le Gall, Pia Neyt, Tommaso M. Boccardi, Marion Grasser, Gernot Längst, Stijn Aesaert, Griet Coussens, Stijn Dhondt, Eveline Van De Slijke, Leonardo Bruno, Jorge Fung-Uceda, Paloma Mas, Marc Van Montagu, Dirk Inzé, Kristiina Himanen, Geert De Jaeger, Klaus D. Grasser, and Mieke Van Lijsebettens

Corresponding author: Mieke Van Lijsebettens
Email: mieke.vanlijsebettens@psb.ugent.be

This PDF file includes:

Supplementary text
Figs. S1 to S6
Tables S1 to S3
SI References

Other supplementary materials for this manuscript include the following:

Dataset S1

www.pnas.org/cgi/doi/10.1073/pnas.1806541116

MATERIALS AND METHODS

Plant material and growth conditions. *hub1-4* (SALK_122512), *spen3-1* (SALK_025388) (1), *spen3-3* (GABI_626H01) (2), *khd1-1* (SALK_046957) (1), *hub1-3* (GABI_276D08) (2), *hub1-4* (SALK_122512) (1), *hub2-1* (GABI_634H04) (2), *khd1-3* (SAIL_1285_H03C1) (3) in Col-0 background were obtained from the Nottingham *Arabidopsis* Stock Centre. T-DNA insertions were confirmed by PCR. A second T-DNA in *spen3-3* (GABI_626H01) was located at the 3' UTR of the *At1g77920* and the 5' end of the *At1g77930* genes, but did not affect their respective gene expression levels (Fig. S4). The *hub1-3 hub2-1* mutant had been described previously (4), whereas the *spen3-1 hub1-4* and *khd1-1 hub1-4* double mutants were constructed in this work and the genotypes were verified by PCR. The clock reporter lines expressing *pCCA1::LUC* (5) and *pTOC1::LUC* (6) were crossed into the *hub1-4*, *spen3-1*, and *khd1-1* mutants and homozygous lines analyzed by *in vivo* luminescence assays. The *p35S::GFP::SPEN3* and *p35S::GFP::KHD1* constructs were obtained by Gateway recombination and were transformed into *Agrobacterium tumefaciens* cells that were used for tobacco (*Nicotiana benthamiana*) leaf infiltration and stable transformation into *Arabidopsis thaliana* (L.) Heynh., accession Columbia-0 (Col-0) by floral dip.

Seedlings were grown in soil (jiffy containers) under growth chamber conditions, namely 16 h day/8 h night with white light and 21°C for flowering time experiments. Seeds for *in vitro* time-lapse analysis on the IGIS platform (7) were sterilized in 3% (v/v) bleach for 15 min and sown on medium containing half-strength Murashige and Skoog (MS) medium (Duchefa), solidified with 0.9% (w/v) plant tissue culture agar (Lab M) on round Petri dishes, stratified for 2 days, then incubated in a growth chamber under long-day conditions (16 h light, 8 h darkness) at 21°C. The average light intensity supplied by cool-white fluorescent tubes (Spectralux Plus 36W/840; Radium) was approximately 60 µmol m^{-2} s^{-1} for *in vitro* and in soil-grown experiments. For bioluminescence assays, plants were stratified for 3 days at 4ºC on plates with MS agar medium and grown for 7 days under 12 h light, 12 h dark cycles with 60 µmol m^{-2} s^{-1} white light at a constant 22ºC temperature. Seedlings were transferred to 96-well plates containing MS agar and 3 mM luciferine (Promega). Luminescence rhythms were monitored under constant white light conditions (60 µmol m-^{2} s-^{1}) with a luminometer LB-960 (Berthold Technologies) and analyzed with the software MikroWin 2000, version 4.34 (Mikrotek Laborsysteme).

Growth parameters and flowering time were also measured by means of an automated weighing, imaging, and watering phenotyping platform, acronym WIWAM XY (www.wiwam.be) according to established protocols (8, 9). WIWAM was placed in an *Arabidopsis* growth room at 21°C, 55% relative humidity, 16 h day/8 h night, and 100 mol m^{-2} s^{-1} light intensity. Seeds were stratified 2 days before sowing in pots with 80-90 g of soil that were randomized by the WIWAM platform. During the entire experiment, the soil water content was set at a constant value of 2.19 g H_2O/g dry soil. Images were acquired for each pot on a daily basis and analyzed. The data were validated with the in-house Interface for Plant Phenotype Analysis (PIPPA) (10).

Circadian clock period calculation. The circadian periods were calculated with the Fast Fourier Transform–Non-Linear Least-squares (FFT-NLLS) suite of the BioDare online data repository (https://biodare2.ed.ac.uk/documents/period-methods) (11). This suite is commonly accepted and

widely used in the circadian community and the method is clearly described on the web page. Essentially, the period estimation is based on curve fitting. FFT NLLS starts with a model with a single cosine and determines the parameters ($\tau 1$, $\phi 1$, $\alpha 1$, and c) by means of a non-linear least squares fitting algorithm. This procedure is repeated with models with additional cosine components (increased N), until addition of a supplemental cosine term does not improve significantly the resulting fit. Once the best model and its parameters have been found, the period is taken to be the period of the cosine component lying within a user-defined range of likely circadian periods (typically 15-35 h).

Bioinformatic analysis. With the PLAZA 2.5 bioinformatic tool, common down- or upregulated genes were classified into significantly overrepresented ($P < 0.05$) gene ontology (GO) classes of the Biological Process type (12).

Multiprobe *in situ* hybridization. Short and specific (GSTs) fragments of the *HUB1* (At2g44950), *SPEN3*(At1g27750), and *KHD1* (At1g51580) genes were cloned in the pGEM-T-Easy vector (Promega). Labeled RNA probes were synthesized by means of *in vitro* transcription in the presence of digoxigenin-11-UTP (*SPEN3* probe), biotin-16-UTP (*KHD1* probe), fluoroscein-12-UTP (*HUB1* probe) and processed as reported (13). Four-day-old *Arabidopsis* Col-0 seedlings were fixed, dehydrated, and handled as described (13). *In situ* hybridization was done with a mix of riboprobes and hybridized by *in situ* whole-mount methodology (13) with minor modifications, namely the hybridization step was carried out overnight at 55°C and the mixture of primary and secondary antibodies was diluted 1:500. Samples were imaged with a Leica inverted TCS SP8 confocal scanning laser microscope. The Alexa fluor dyes were detected simultaneously by combining the settings indicated in the sequential scanning facility of the microscope.

Root growth analysis. Root growth was measured on seedlings grown vertically on half-strength MS medium supplemented with 1% (w/v) sucrose, 0.8% (w/v) plant tissue culture agar (Lab M), pH 5.7, at 21°C under 24-h light conditions (75 $\mu mol\ m^{-2}\ s^{-1}$). The root meristem size was determined 5 days after germination (DAG) as the number of cells in the cortex cell file from the quiescent center to the first elongated cell (14). The samples were mounted with clearing solution (80 g chloral hydrate, 30 ml glycerol, and 10 ml dH_2O) and observed immediately. Root length was marked at 10 DAG and measured with the ImageJ software (http://rsbweb.nih.gov/ij/). Means between samples were compared by a two-tailed Student's *t*-test and variances with an ANOVA.

Tandem Affinity Purification. TAP (15) or GS (16) tags were fused N-terminally to full length cDNAs of HUB1, HUB1pm, and HUB2, and C-terminally to SPEN3. In the HUB1pm, two cysteines of the RING domain (positions 826 and 829) were replaced by serines. The TAP-tagged HUB1 proteins were enzymatically active and complemented partially the *hub1-1* mutation (4). Tagged transgenes were expressed under the control of the constitutive cauliflower tobacco mosaic virus 35S promoter and transformed in *Arabidopsis* cell suspension cultures (17). Protocols of proteolysis and peptide isolation, acquisition of mass spectra by a 4800 Proteomics Analyzer (Applied Biosystems), and mass spectrometry-based protein homology identification based on the TAIR genomic database, were as described (18). Experimental background proteins

were subtracted based on approximately 40 TAP experiments on wild-type cultures and cultures expressing the TAP-tagged mock proteins GUS, RFP, and GFP (18).

Production of recombinant proteins. The RRM domain-containing region of SPEN3 and the two KH domain-containing region of KHD1 were amplified by PCR with *HiFi* DNA polymerase (KAPA Biosystems) and the iProof high-fidelidy PCR kit (Bio-Rad), respectively, with an *Arabidopsis* cDNA library as template and primers providing the required restriction enzyme cleavage sites (Table S3). The amplified PCR fragment of SPEN3 was digested with *Bam*HI/*Sal*I and cloned into the *Bam*HI/*Sal*I-digested *E. coli* expression plasmid pGEX-5X-1 (GE Healthcare), providing an N-terminal GST with the pGEX-5X-1-RRM-SPEN3 plasmid for the RRM domain of SPEN3 as a result. The obtained PCR fragment of KHD1 was digested with *Bam*HI/*Sal*I and cloned into the *Bam*HI/*Sal*I-digested *E. coli* expression plasmid pQE9 (Qiagen), providing an N-terminal 6×His-tag, resulting in the pQE9-KHD1-N plasmid for the N-end part of KHD1 that contains two KH domains. Plasmid constructions were checked by DNA sequencing. For protein production, the pGEX-5X-1-RRM-SPEN3 expression vector was transformed into *E. coli* BL21+pRARE cells. After induction by 1 mM isopropyl β-D-1-thiogalactopyranoside (IPTG; Sigma-Aldrich), the GST-tagged RRM-SPEN3 was purified by glutathione-sepharose affinity chromatography as previously described (19). *E. coli* M15 cells were transformed with the pQE9-KHD1-N expression vector. After induction by 1 mM IPTG, the 6×His-tagged KHD1-N was purified by metal-chelate chromatography with Ni-NTA agarose (Qiagen) from *E. coli* lysates essentially as described previously (20). By means of PD10 columns (Pharmacia), the purified proteins were collected in buffer (10 mM phosphate buffer, pH 7.0, 1 mM EDTA, 1 mM dithiothreitol [DTT], and 0.5 mM phenylmethanesulfonyl fluoride [PMSF; Sigma-Aldrich]) and the recombinant proteins were analyzed by sodium dodecyl sulfate-polyacrylamide gel electrophoresis (SDS-PAGE) and mass spectrometry.

Fluorescent Electrophoretic Mobility Shift Assay (EMSA) binding. RNA binding of the recombinant proteins was examined by EMSA as described (20) with fluorescently labeled ssRNA oligonucleotides (Table S3) (21) used before to study general RNA interactions of various *Arabidopsis* proteins (20, 21). Different protein concentrations were incubated for 15 min with the Cy3-labeled ssRNA (25 nM) probe in binding buffer (10 mM Hepes, pH 7.9, 3% [w/v] Ficoll, 10 mM $MgCl_2$, 5 mM KCl, 200 mM NaCl, 1 mM EDTA, 0.5 mM DTT, 1 mM spermidine, 0.1 mg/ml bovine serum albumin). Binding reactions were analyzed in 1× Tris/borate/EDTA (TBE) polyacrylamide gels. The RNA was visualized by imaging with a Typhoon 8600 instrument (GE Healthcare). Competition assays were done with constant protein concentrations (3 µM) and labeled ssRNA probes and increasing concentrations of unlabeled ssRNA or ssDNA.

Fluorescent MicroScale Thermophoresis (MST) binding assay. MST binding experiments were carried out essentially as previously described (20) with 200 nM 25-nucleotide-long Cy3-labeled ssRNA or ssDNA oligonucleotides. MST measurements were done in protein buffers with a protein concentration range at 40% MST power, 50% LED power in standard capillaries at 25°C on a Monolith NT.115 device (NanoTemper Technologies). The data were analyzed with the MO.Affinity Analysis software (V2.3, NanoTemper Technologies) and binding reactions were determined by examining Temperature Related Intensity Changes (TRIC effect). To calculate the fraction bound, the ΔF_{norm} value of each point was divided by the amplitude of the

fitted curve, resulting in values from 0 to 1 (0 = unbound, 1 = bound), and processed with the KaleidaGraph 4.5 (Synergy Software).

RNA methods. RNA was isolated with the RNeasy Plant Kit (Qiagen) with on-column DNase digestion. The manufacturer's protocol was modified by two additional washes of RNeasy spin columns with RPE buffer. Complementary DNA (cDNA) was synthesized with the SuperScript III First-strand Synthesis Kit (Life-Invitrogen, CAT. 18080051).

Real-time PCR was run in technical triplicates with the LightCycler 480 SYBR Green I Master (Roche Life Science) and the Janus robot (PerkinElmer) for pipetting. The LightCycler 480 Real-Time PCR System was used for amplification (95°C for 10 min, 45 cycles of 95°C/10 s, 60°C/15 s, 72°C/30 s followed by a melting curve analysis). The qPCR results were analyzed with the qBase Plus software (Biogazelle). The PP2A (At1g13320) and UBC (At5g25760) genes were used as references for gene expression normalization. The primer sequences used are presented in Table S3. For the transcriptome**,** RNA was extracted from shoot apices of 10-day-old seedlings. The A260/A280 and the A260/A230 ratios were measured with a NanoDrop spectrophotometer (Thermo Fisher Scientific) to evaluate the quantity and purity of the samples. Additionally, the high RNA quality was verified by means of the Agilent Bioanalyzer system. After the library preparation by TruSeq, RNA was sequenced on the Illumina HiSeq. Normalization statistics, and bioinformatics were carried out on the raw data to allow pairwise differential gene expression analyses (Nucleomics Core Facility, VIB, Leuven, Belgium). The Gene Ontology categories of the differentially expressed genes were identified with the PLAZA 2.5 software (12).

ChIP-qPCR. The isolated chromatin was sonicated in a Vibra-cell sonicator (Sonics & Materials) with four 15-s pulses at a 20% amplitude and immunoprecipitated with 5 µg of H2Bub antibodies (Medimabs, MM-029). Protein A Agarose (Millipore) was used to collect immunoprecipitated chromatin. After reverse cross-linking and proteinase K digestion, DNA was purified with the MinElute PCR Purification Kit (Qiagen) and eluted with the elution buffer supplemented with RNaseA (10 µg/ml). Samples were analyzed by real-time qPCR with primers in the promoter and coding regions of the *FLC* (22) and *CCA1* (Table S3) genes. The amount of immunoprecipitated DNA was calculated relative to the input.

Yeast Two-Hybrid Analysis. Constructs used for Y2H were obtained by cloning cDNAs of the HUB1, HUB2, SPEN3, SPEN3 N-terminus (761 amino acids, including RRM domain), and SPEN3 C-terminus (488 amino acids, including SPOC domain) by the Gateway Technology (Life Technologies). Constructs were introduced by an LR recombination into the pDEST^{tm}22 and pDEST^{tm}32 destination vectors, resulting in fusions to the GAL4 activation domain (AD) and GAL4-binding domain (BD), respectively (ProQuest^{TM} Two-HybridSystem, Life Technologies). All plasmids were transformed into yeast strains with the opposite mating types MaV203 MATa and MATα. Transformed yeast strains were selected for the presence of pDEST22 or the pDEST32 vector.

Transformed yeast strains were selected for the presence of pDEST22 or the pDEST32 vector and the abundance of the fusion proteins was assessed by Western-blot. Self-activation of both bait and prey constructs were tested by yeast transformation for non-PREY-specific activation of reporter gene expression by BAIT-constructs or BAIT-GAL-4-DNA-independent activation exerted by PREY constructs in a colony-lift filter assay with X-Gal as substrate. Fusion

proteins that showed self-activation, *i.e.*, HUB2 and KHD1, were omitted from the pairwise screens. Diploid transformants were tested for positive interactions by growing the mating strains in SD-leucine-tryptophan-histidine medium with increasing concentrations (0 mM, 3 mM, and 10 mM) of 3-amino-1,2,4-triazole (3-AT) to assess the interaction strengths. Constructs of known interacting proteins, DmDP and DmE2F, were used as the positive control and the negative control consisted of yeast strains containing an empty AD vector mated with the BD fusion of the protein of interest. For each interaction, three independent biological repeats were done and for the assays the TECAN Genesis Automation and TECAN TEMO-96 pipetting robot were used (TECAN, Munich, Germany).

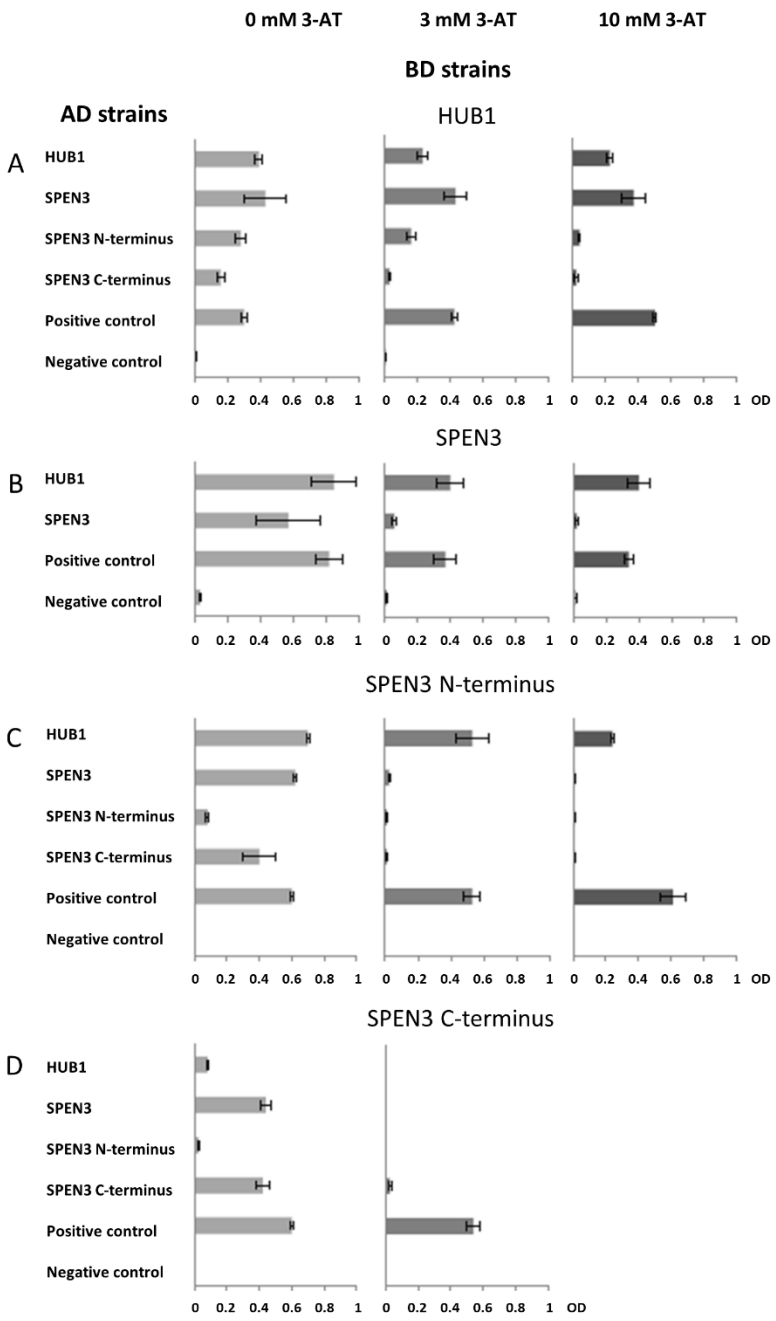

Fig. S1. Yeast two-hybrid interactions between HUB1, SPEN3, SPEN3 N-terminus, and SPEN3 C-terminus.

The yeast strains expressing the HUB1, SPEN3, SPEN3 N-terminus, and SPEN3 C-terminus proteins fused to the activation domain (AD strains, ordinate) or binding domain (BD strains, panels *A*-*D*) did not show self-activation and were mated pairwise to test for direct interactions between proteins that allowed yeast growth on selective medium and quantification as the optical density (OD_{600}) of the culture. Different concentrations (0 mM, 3 mM, and 10 mM) of 3-amino-1,2,4-triazole (3-AT) were applied to the medium to detect the high-affinity binding between two interactors allowing yeast to survive increased 3-AT concentrations. For each interaction, the average of three independent biological repeats are shown. As a positive control, known interactors (DmDP and DmE2F) were used and, as negative control, the empty AD vector strain was mated with the BD fusion of the protein of interest.

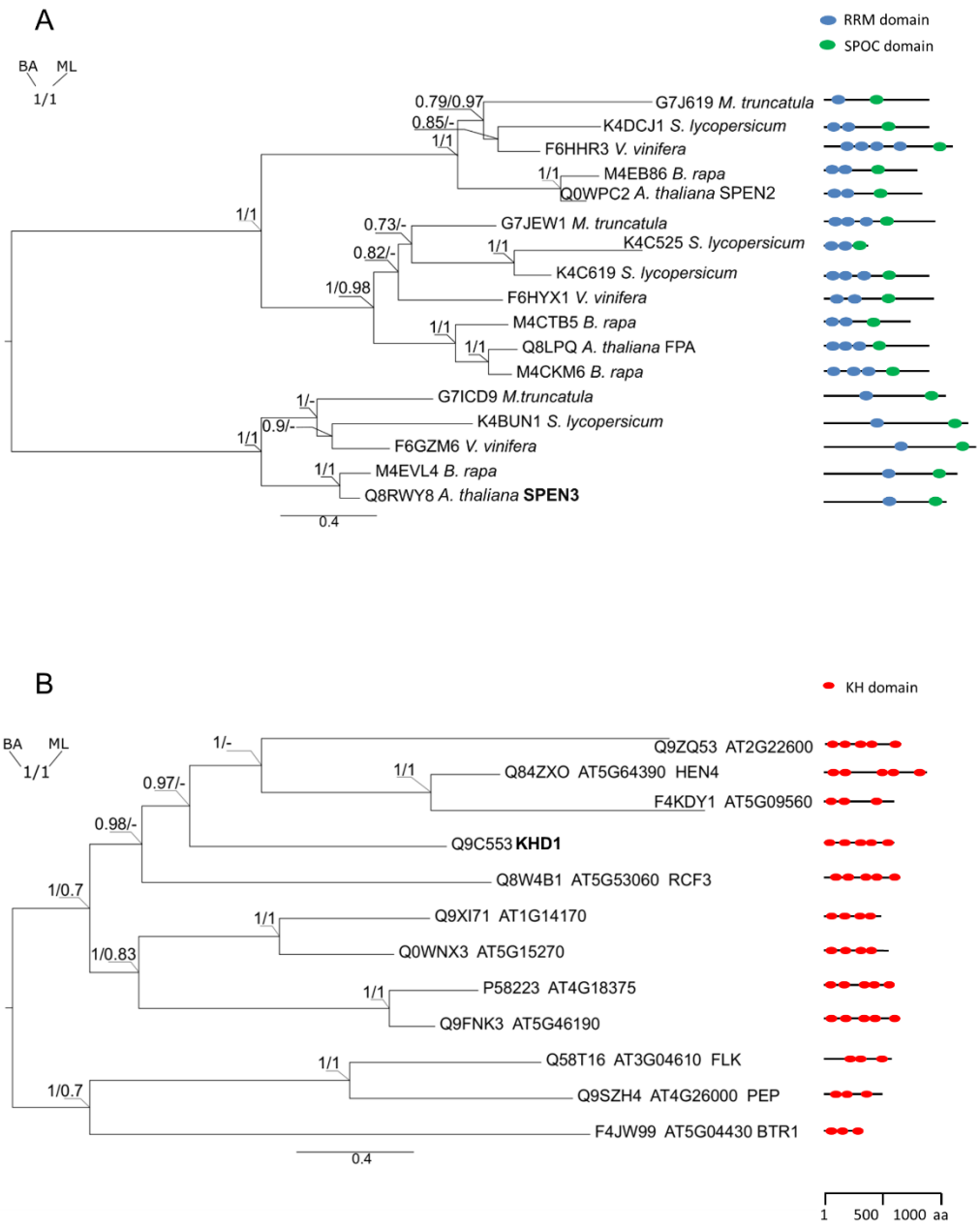

Fig. S2. Evolutionary relationships of SPEN3 (*A*) and KHD1 (*B*) proteins over taxa and within *Arabidopsis thaliana*. The evolutionary history was inferred from two independent maximum likelihood (ML) and Bayesian approaches (BA) with PhyML (23, 24) and MrBayes 3.2.6 (25), respectively. Both trees were estimated with a best-fit model obtained by MEGA X (26) as JTT + G for SPEN3 (*A*) and LG + G for KHD1 (*B*). The analysis involved 17 (*A*) and 12 (*B*) amino acid sequences retrieved from the UniProt database. In MrBayes, two independent runs were applied and trees were sampled every 200th generation for 5 000 000 generations (with a 25% burn-in). Overall, deviation of split frequencies for all trees used for consensus was much below 0.01. The reliability of the nodes is indicated by their posterior probability values (BA) and bootstrap values (1000 replicates) (ML) presented along the nodes. Node support values below 70% were not shown. The scale bar represents the genetic distance.

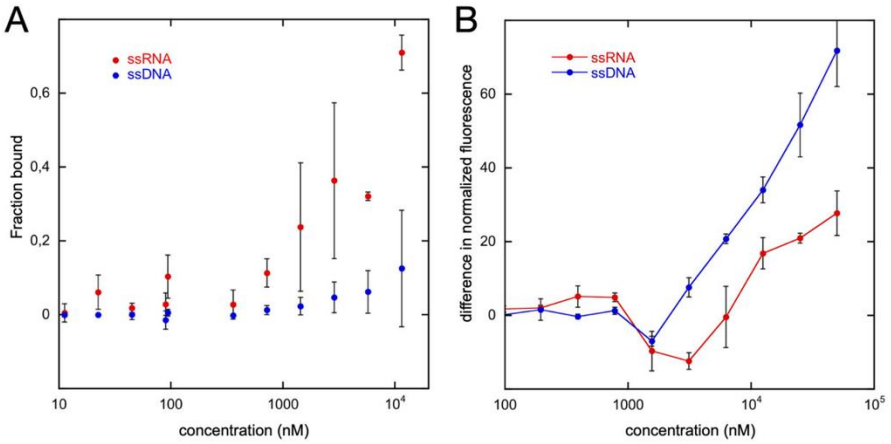

Fig. S3. MST analysis of SPEN3 and KHD1 interactions with nucleic acids.
(*A*) Increasing concentrations of the GST-RRM-SPEN3 protein incubated with 200 nM of 25-nucleotide-long ssRNA or ssDNA of the same sequence. Protein-nucleic acid interactions were quantified by MST. The approximate bound fraction of nucleic acids per tested protein concentration is plotted. (*B*) Increasing concentrations of binding of 6×His-KHD1-N protein incubated with ssRNA and ssDNA as in (*A*). Protein-nucleic acid interactions were measured by MST. In case of 6×His-KHD1-N binding to ssRNA and ssDNA, the MST analysis revealed a complex pattern of changes in the thermophoretic mobility of the interacting molecules. Instead of following a typical binding curve with increasing protein concentrations, a significant change in the mobility direction at a protein concentration of 1 µM. At lower concentrations, the protein-nucleic acid complexes moved toward the heated region in the capillary, whereas at higher concentrations (above 4 µM) they left the heated region. This behavior resulted in a "local minimum" of the plotted data that can be interpreted as two dependent binding events, creating two different protein-nucleic acid complexes with different thermophoretic behaviors established each one after the other with increasing protein concentration. The overlay of the thermophoretic properties can result in such plots. As no K_D or Hill fitting could be applied, the curves can only be described in a qualitative manner. The plot is displayed as changes in normalized fluorescence exhibiting qualitative differences in the presence of RNA or DNA. The "local minimum" was much more pronounced in the presence of RNA and the curve reached a plateau at high protein concentrations. In contrast, in the presence of DNA, the curve did not reach a plateau, hinting at partial DNA binding. Hence, this qualitative analysis supports the EMSA experiments, suggesting improved RNA binding. Measurements were done with three biological and three technical replicates. Error bars indicate standard deviation of the biological replicates.

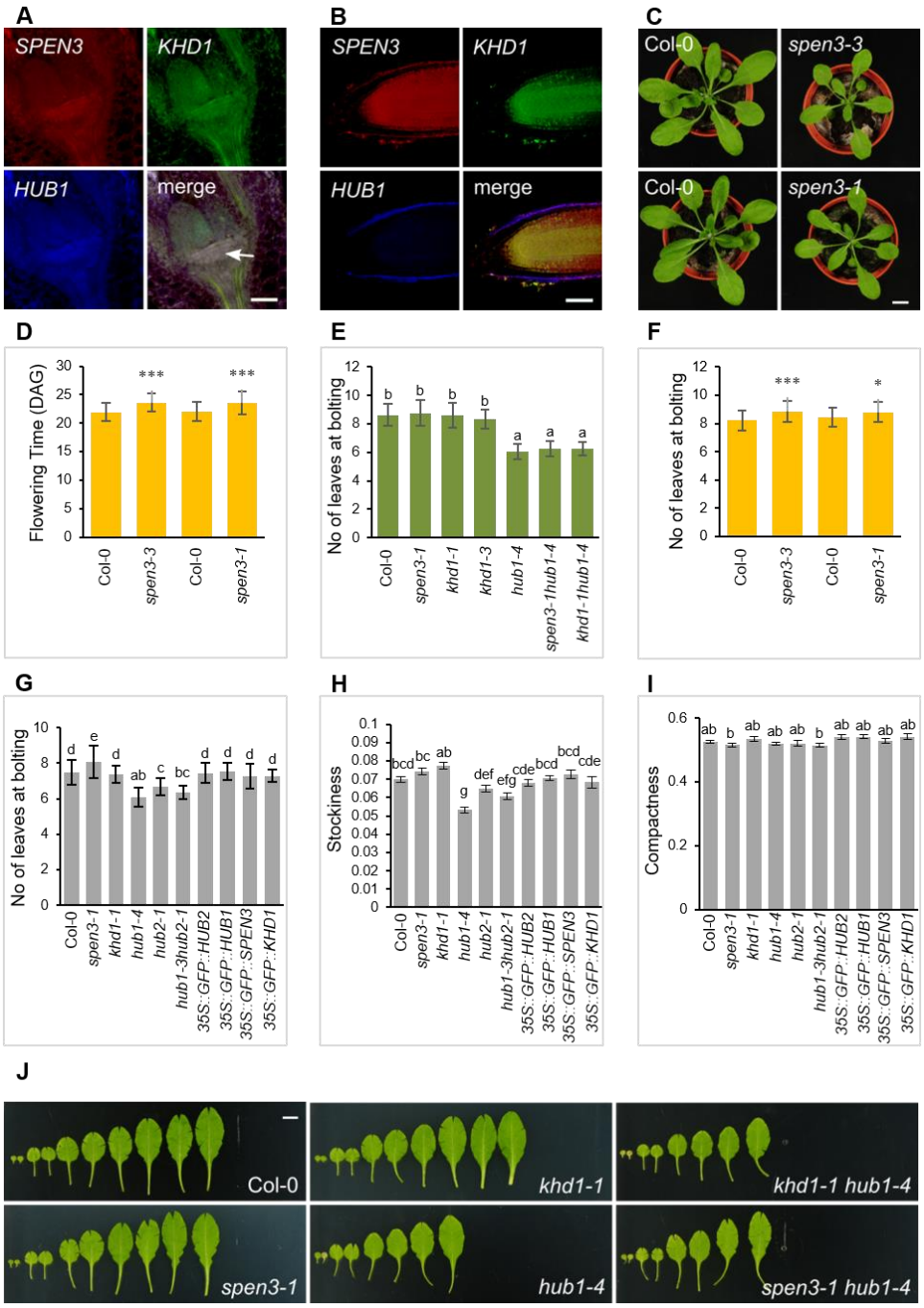

Fig. S4. *in situ* hybridization and leaf phenotypes of mutants and overexpression lines.
(*A* and *B*) Whole-mount, multiprobe *in situ* hybridization of the shoot apex (*A*) and the primary root meristem (*B*). Arrow indicates white-pink merge of *HUB1* (blue samples treated with HUB1 FITC riboprobe and rabbit anti-FITC followed by AF647 chicken antirabbit), *SPEN3* (red samples treated with *SPEN3* Dig-riboprobe and sheep anti-Dig, followed by AF555 Donkey anti-sheep), and *KHD1* (green samples treated with *KHD1* Bio-riboprobe and mouse anti-Bio followed by AF488-Donkey anti-mouse IgG) expression pattern in the shoot apex. (*C*) Rosette phenotype of the *spen3-3* and *spen3-1* alleles and their Col-0 controls at 25 DAG. (*D*) Flowering time of *spen3-3* and *spen3-1* and their Col-0 controls grown in jiffy pots (n = 50). (*E*) Number of rosette leaves per seedling at bolting in jiffy pots (n = 51). (*F*) Number

of rosette leaves per seedling at bolting in jiffy pots ((*n* = 50). (*G*) Number of rosette leaves per seedling at bolting grown in the WIWAM-automated platform (*n* = 24). (*H*) Stockiness and (*I*) compactness of the rosettes in WIWAM experiment calculated at 23 DAS. (*J*) Leaf series of 26 DAG seedlings grown in jiffy container experiment. Control, Col-0; single mutants, *spen3-1*, *khd1-1* and *hub1-4*; double mutants, *spen3-1 hub1-4* and *khd1-1 hub1-4*. Error bars represent standard deviations. Ordinary one-way ANOVA with 95% confidence shows a significant difference between the genotypes, represented by the letters (panels *E,G,H,I*). Asterisks (*D* and *F*) indicate statistically significant differences by Student's *t*-test (**P* < 0.05, ****P* < 0.001).

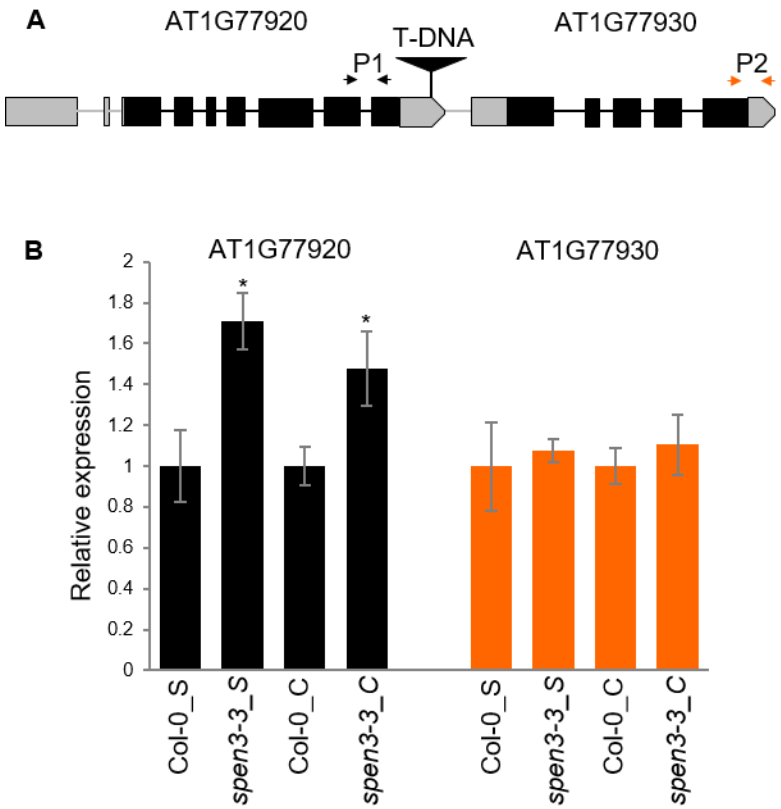

Fig. S5. Expression levels of genes flanking the second T-DNA insertion in *spen3-3*.
(*A*) Scheme of a second T-DNA insertion at the 3' end of *At1g77920* and the 5' end of *At1g77930* in the *spen3-3* allele. (*B*) qPCR analysis of *At1g77920* and *At1g77930* gene expression levels in seedling (S) and cauline (C) leaf tissue of *spen3-3* and Col-0 control (primers, see Table S3), five biological replicates. Asterisks indicate statistically significant differences by Student's *t*-test (* $P < 0.05$)

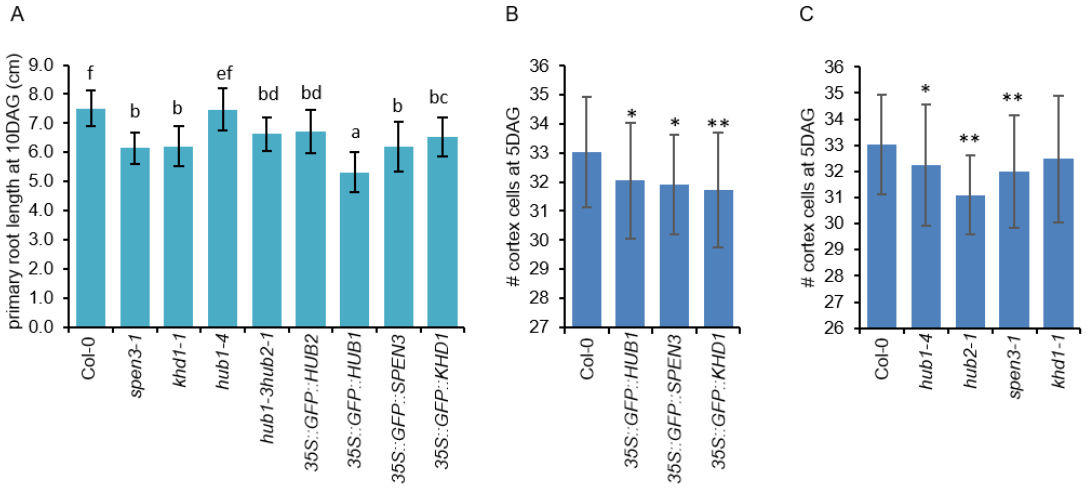

Fig. S6. Primary root phenotypes of mutants and overexpression lines.
(*A*) Primary root length at 10 DAG ($n \geq 15$). (*B* and *C*) Root meristem size measured by the number of cortex cells of 5 DAG seedlings of overexpression lines ($n > 15$) (*B*) and mutant lines ($n \geq 10$) (*C*). Error bars represent standard deviations. Ordinary one-way ANOVA with 95% confidence shows a significant difference between the genotypes, represented by the letters (panel *A*). Asterisks (panels *B* and *C*) indicate statistically significant differences by Student's *t*-test (*$P < 0.05$, **$P < 0.01$).

Table S1. AGI codes of the 117 DEGs common to the *hub1-4*, *khd1-1*, and *spen3-1* transcriptomes ($log_2FC \geq 0.5$ or $log_2FC \leq -0.5$, $P \leq 0.05$)

Gene ID	Gene name	Function/process	*hub1-4* vs COL-0: log_2 FC	*khd1-1* vs COL-0: log_2 FC	*spen3-1* vs COL-0: log_2 FC
AT3G30720	QQS	Starch biosynthetic process	-5.6626	-5.5745	-6.5275
AT4G08093	NA	Unknown	-3.7844	-5.5504	-4.0931
AT2G01422	NA	Unknown	-3.3395	-3.7738	-2.5119
AT4G04223	NA	Unknown	-3.1981	-2.3271	-3.6096
AT4G15320	ATCSLB06	Cellulose biosynthetic process	-1.9482	-2.2482	-2.0571
AT1G48740	F11I4_9	Oxidation reduction process	-1.7234	-1.2481	-1.8338
AT1G51055	NA	Unknown	-1.4514	-1.3610	-1.3864
AT1G55320	AAE18	Auxin metabolic process	-1.2355	-0.8119	-0.6587
AT4G08991	NA	Unknown	-1.2329	-1.9179	-1.3986
AT5G25970	T1N24.19	Transferase activity	-1.1978	-0.8172	-1.1685
AT5G07640	NA	Zinc ion binding	-1.1420	-0.9536	-0.9802
AT2G39460	ATRPL23A	RNA binding	-1.0806	-1.0022	-0.6850
AT3G05727	NA	Unknown	-0.9690	-0.6627	-1.0264
AT2G29570	PCNA2	DNA methylation	-0.9243	-0.7950	-0.5766
AT3G55660	ATROPGEF6	Unknown	-0.8981	-0.6359	-0.5877
AT5G22440	RPL10AC	RNA methylation	-0.8793	-0.8620	-0.7202
AT5G37010	NA	DNA replication	-0.8736	-0.7098	-0.4696
AT1G52770	F14G24.4	Response to light stimulus	-0.8589	-1.3647	-0.8099
AT3G16490	IQD26	Calmodulin binding	-0.8390	-0.8087	-0.8740
AT2G25880	AtAUR2	Histone kinase	-0.8332	-0.8656	-0.5894
AT2G28620	NA	DNA replication	-0.8305	-0.7375	-0.5404
AT2G01020	NA	Peptide biosynthetic process	-0.7982	-0.9755	-0.8181
AT2G33400	F4P9.17	Unknown	-0.7936	-0.5135	-0.6040
AT1G18370	HIK	Microtubule movement	-0.7906	-0.6073	-0.6042
AT5G01600	ATFER1	Iron ion binding	-0.7852	-1.0765	-0.6556
AT4G02800	T5J8.12	Microtubule cytoskeleton	-0.7802	-0.6539	-0.5214
AT4G03100	F4C21.2	Microtubule cytoskeleton	-0.7608	-0.8148	-0.5114
AT1G02780	emb2386	RNA methylation	-0.7545	-0.6800	-0.9208
AT3G23890	TOPII	DNA topoisomerase	-0.7470	-0.5620	-0.5724
AT4G35810	NA	Oxidation reduction process	-0.7201	-0.7203	-0.9608
AT3G01710	NA	Unknown	-0.7187	-0.5457	-0.5202
AT4G22505	NA	Lipid transport	-0.6991	-0.5741	-0.8263
AT5G38940	NA	Response to salt stress	-0.6947	-0.7681	-1.0002
AT2G38620	CDKB1	Regulation of cell cycle	-0.6756	-0.5173	-0.7126
AT5G15200	RPS9B	RNA methylation	-0.6751	-0.5741	-0.6052
AT3G58650	F14P22.240	DNA replication	-0.6746	-0.6901	-0.6336
AT5G60150	NA	Petal formation	-0.6702	-0.7296	-0.5222
AT1G05440	NA	DNA methylation	-0.6700	-0.7066	-0.5283
AT5G44560	VPS2.2	Protein binding	-0.6659	-0.5251	-0.5011
AT2G26760	CYCB1	Regulation of cell cycle	-0.6633	-0.7223	-0.6465
AT1G23790	F5O8.34	Cell proliferation	-0.6442	-0.7267	-0.5978
AT3G26050	NA	Unknown	-0.6299	-0.6320	-0.5259
AT5G67270	ATEB1C	Microtubule binding	-0.6257	-0.6774	-0.6385
AT3G19050	POK2	Microtubule movement	-0.6187	-0.5180	-0.5445
AT5G26742	emb1138	Embryo development	-0.5808	-0.9022	-0.6706
AT2G36885	NA	Unknown	-0.5808	-0.8775	-0.8374
AT4G24670	TAR2	Cotyledon development	-0.5388	-0.6692	-0.6080
AT2G45490	AtAUR3	Histone kinase	-0.5322	-0.5612	-0.7462
AT2G33560	BUBR1	Cell proliferation	-0.5258	-0.6428	-0.5698
AT4G37490	CYC1	Regulation of cell cycle	-0.5244	-0.7092	-0.6084
AT5G35935	NA	Transposon	3.8585	4.0484	3.9318
AT1G19510	ATRL5	Regulation of transcription	2.6802	1.7416	1.6497
AT3G10420	SPD1	Nucleoside-triphosphatase activity	2.4560	2.4592	2.6330
AT3G05660	AtRLP33	Kinase activity	2.4204	1.4367	1.4173
AT4G08040	ACS11	Biosynthetic process	1.8670	0.9910	1.2030
AT2G34010	T14G11.13	Negative regulation of transcription	1.7997	1.0896	0.8731
AT1G51820	NA	Proline transport	1.6036	1.9470	1.5766
AT2G26560	PLP2	Lipase activity	1.5401	1.4479	1.6085
AT1G43910	F9C16_7	Response to ABA stimulus	1.4203	1.3555	1.1442
AT3G16030	CES101	Immune response	1.3967	1.1568	1.0114
AT4G36280	CRH1	ATP binding	1.2300	0.7077	0.5734
AT5G15510	NA	Cell proliferation	1.1310	0.7409	1.2072
AT5G17860	CAX7	Transmembrane transport	1.1310	0.7409	1.2072

AT1G62510	NA	Lipid transport	1.1214	0.9785	0.8740
AT5G38970	BR6OX1	Oxidation reduction process	1.1193	1.2404	1.2257
AT1G52880	NAM	Regulation of transcription	1.1080	0.7682	0.9576
AT4G11900	NA	Protein phosphorylation	1.0676	0.7431	0.7588
AT3G53250	T4D2.180	Response to auxin stimulus	1.0341	0.9364	0.7971
AT3G62860	F26K9_290	Catalytic activity	1.0282	1.0083	0.7175
AT1G72430	T10D10.10	Response to auxin stimulus	0.9981	1.0623	0.8578
AT1G21270	WAK2	Oligosaccharide metabolic process	0.9727	0.7971	0.6735
AT5G64780	NA	Unknown	0.9604	0.6438	0.5608
AT2G39980	NA	Response to karrikin	0.9578	0.6103	0.5734
AT3G61430	PIP1A	Water channel activity	0.9367	0.7735	0.5416
AT4G18010	IP5PII	Inositol tri-phosphate metabolic process	0.8834	1.2286	0.6841
AT3G56000	ATCSLA14	Transferase activity	0.8726	0.9119	0.7815
AT3G48720	T8P19.230	Cutin biosynthetic process	0.8433	0.8613	0.6017
AT5G08150	SOB5	Cytokinin metabolism process	0.8382	1.1877	0.6384
AT1G23130	T26J12.10	Defense response	0.8248	0.9054	0.6017
AT3G12090	TET6	Transition metal ion transport	0.8139	0.6686	0.6863
AT5G24030	SLAH3	Nitrate transport	0.7619	0.9383	0.6074
AT2G31730	BHLH-BETA	Response to ethylene and GA stimulus	0.7106	0.8444	0.6729
AT5G07000	ATST2B	Sulfotransferase activity	0.6955	0.9848	0.6295
AT3G07340	BHLH62	Regulation of transcription	0.6624	0.6468	0.5896
AT4G23190	CRK11	Kinase activity	0.6350	0.7084	0.8002
AT5G23750	MRO11.3	Cell wall biogenesis	0.5664	0.6600	0.7512
AT4G32790	F4D11.10	Catalytic activity	0.5664	0.5992	0.5092
AT2G41330	NA	Cell redox homeostasis	0.5613	0.6276	0.7785
AT2G23690	NA	Protein myristoylation	0.5438	0.7003	0.8397
AT1G02820	F22D16.18	Embryo development	-1.7547	-1.2409	1.2362
AT1G62540	FMO GS-OX2	Oxidation reduction process	-1.4021	-0.9912	0.9452
AT4G26790	NA	Lipid metabolic process	-1.1570	-1.1056	0.8255
AT3G21670	NRT1.3	Oligopeptide transport	-1.1033	-1.0078	0.9084
AT1G16730	UP6	Fatty acid beta oxydation	-1.0651	-1.2906	1.0012
AT4G37310	CYP81H1	Oxidation reduction process	-1.0019	-0.7621	0.5620
AT2G46680	ATHB-7	Regulation of transcription	-0.9295	-0.6854	0.6970
AT1G73390	T9L24.40	Protein myristoylation	-0.9262	-0.6509	0.6113
AT2G17300	NA	Unknown	-0.7890	-0.5806	0.5410
AT5G03760	ATCSLA09	Calcium ion transport	-0.7349	-0.7330	0.7095
AT5G61290	NA	Oxidation reduction process	-0.6413	-0.7854	0.7625
AT1G64770	NDF2	Carbohydrate metabolic process	-0.5301	-0.5406	0.5175
AT4G37770	ACS8	Biosynthetic process	1.7545	2.0780	-1.8580
AT4G40065	NA	Unknown	1.4381	1.1595	-1.3468
AT2G23170	GH3.3	Response to auxin stimulus	1.4334	1.2295	-0.7410
AT2G18010	SAUR10	Response to auxin stimulus	1.3172	1.5038	-1.1684
AT3G42800	T21C14_20	Unknown	1.1613	1.4009	-0.8314
AT1G04610	YUC3	Oxidation reduction process	0.8388	1.2292	-1.9934
AT1G30420	ATMRP12	Transmembrane transport	0.5738	0.5111	-1.0747
AT1G51830	T14L22.4	Nitrate transport	-1.5491	1.2138	-1.0585
AT4G20320	F1C12.230	Pyrimidine nucleotide biosynthetic process	-1.4217	-0.8890	-0.5056
AT4G30170	PER45	Oxidation reduction process	-1.2226	1.4707	-1.1787
AT3G32925	NA	Transposon	2.4493	-2.0186	1.4498
AT5G59670	NA	Protein phosphorylation	1.2640	-1.1608	1.5756
AT1G73000	PYL3	Unknown	1.2088	-1.0563	1.6080
AT1G11070	NA	Unknown	0.9290	-0.6423	0.8314
AT1G78000	SULTR1	Nitrate transport	-1.5906	0.6725	0.8204
AT3G54160	F24B22.120	Unknown	0.9710	-1.2585	-1.0686

*P values for all $\log_2 FC \leq 0.05$.

Table S2. PLAZA enrichment of Biological Process Gene Ontology (GO) categories identified within genes down- or upregulated in the indicated mutants. For the single mutants, only the mutant-specific down- or upregulated genes are presented. The GO ratio is the ratio between the number of analyzed annotated genes that belong to the given GO category and the number of all analyzed annotated genes.

GO term	Log2-Enrichment	*P* value	GO ratio (%)	Description
Down-regulated in *hub1-4, khd1-1,* and *spen3-1*				
GO:0051726	4.63	5.67E-04	12	Regulation of cell cycle
GO:0016572	8.32	4,.0E-03	5	Histone phosphorylation
GO:0007049	3.40	3.00E-02	12	Cell cycle
Down-regulated in *hub1-4* and *spen3-1*				
GO:0051726	3.71	2.00E-02	6	Regulation of cell cycle
GO:0016572	7.40	3.00E-02	2	Histone phosphorylation
Down-regulated in *hub1-4* and *khd1-1*				
GO:0008152	0.54	4.52E-17	61	Metabolic process
GO:0019748	2.13	4.61E-16	9	Secondary metabolic process
GO:0006260	3.09	9.67E-13	4	Cellular DNA replication
GO:0006259	2.22	1.73E-12	7	Cellular DNA metabolic process
GO:0044238	0.53	6.76E-12	51	Primary metabolic process
GO:0044237	0.53	3.52E-11	49	Cellular metabolic process
GO:0044281	1.24	4.94E-11	16	Small molecule metabolic process
GO:0006519	1.76	9.67E-11	9	Cellular amino acid and derivative metabolic process
GO:0016144	3.62	1.52E-10	3	*S*-glycoside biosynthetic process
GO:0019758	3.62	1.52E-10	3	Glycosinolate biosynthetic process
GO:0019761	3.62	1.52E-10	3	Glucosinolate biosynthetic process
GO:0009812	3.23	1.64E-10	3	Flavonoid metabolic process
GO:0009987	0.42	2.07E-10	60	Cellular process
GO:0009813	3.30	2.84E-10	3	Flavonoid biosynthetic process
GO:0009058	0.70	4.05E-10	33	Biosynthetic process
GO:0034637	2.36	6.90E-10	5	Cellular carbohydrate biosynthetic process
GO:0044249	0.70	8.93E-10	33	Cellular biosynthetic process
GO:0044283	1.59	3.03E-09	9	Small molecule biosynthetic process
GO:0009698	2.50	3.42E-09	4	Phenylpropanoid metabolic process
GO:0006807	0.79	4.56E-09	26	Nitrogen compound metabolic process
GO:0016137	2.62	4.79E-09	4	Glycoside metabolic process
GO:0016138	3.07	5.27E-09	3	Glycoside biosynthetic process
GO:0016143	2.92	8.79E-09	3	S-glycoside metabolic process
GO:0019757	2.92	8.79E-09	3	Glycosinolate metabolic process
GO:0019760	2.92	8.79E-09	3	Glucosinolate metabolic process
GO:0009699	2.63	1.12E-08	4	Phenylpropanoid biosynthetic process
GO:0042398	2.26	5.03E-08	5	Cellular amino acid derivative biosynthetic process
GO:0019438	2.21	5.06E-08	5	Aromatic compound biosynthetic process
GO:0006725	1.87	5.39E-08	6	Cellular aromatic compound metabolic process
GO:0006790	2.25	5.93E-08	5	Sulfur metabolic process
GO:0016051	2.07	9.32E-08	5	Carbohydrate biosynthetic process
GO:0007049	2.14	1.47E-07	5	Cell cycle
GO:0006575	2.00	1.50E-07	5	Cellular amino acid derivative metabolic process
GO:0044272	2.73	2.87E-07	3	Sulfur compound biosynthetic process
GO:0005975	1.21	2.53E-06	10	Carbohydrate metabolic process
GO:0050896	0.61	2.58E-06	29	Response to stimulus
GO:0044262	1.49	6.89E-06	7	Cellular carbohydrate metabolic process
GO:0022402	2.31	1.22E-05	3	Cell cycle process
GO:0042440	2.48	1.22E-05	3	Pigment metabolic process
GO:0043455	3.52	1.31E-05	2	Regulation of secondary metabolic process
GO:0010439	5.36	2.42E-05	1	Regulation of glucosinolate biosynthetic process
GO:0000103	4.34	2.64E-05	1	Sulfate assimilation
GO:0006791	4.18	6.57E-05	1	Sulfur utilization
GO:0006261	3.08	6.78E-05	2	DNA-dependent DNA replication
GO:0034285	2.85	1.07E-04	2	Response to disaccharide stimulus
GO:0006270	4.51	1.23E-04	1	DNA replication initiation
GO:0006950	0.71	1.68E-04	19	Response to stress
GO:0046148	2.45	3.03E-04	3	Pigment biosynthetic process
GO:0006281	2.07	3.43E-04	3	DNA repair

GO:0034984	2.07	3.67E-04	3	Cellular response to DNA damage stimulus
GO:0009744	2.82	4.69E-04	2	Response to sucrose stimulus
GO:0043255	4.78	4.79E-04	1	Regulation of carbohydrate biosynthetic process
GO:0044271	1.57	4.94E-04	5	Cellular nitrogen compound biosynthetic process
GO:0006139	0.66	5.11E-04	19	Cellular nucleobase, nucleoside, nucleotide, and nucleic acid metabolic process
GO:0006974	2.01	6.27E-04	3	Response to DNA damage stimulus
GO:0009309	2.01	6.27E-04	3	Amine biosynthetic process
GO:0010675	4.62	9.38E-04	1	Regulation of cellular carbohydrate metabolic process
GO:0009753	1.90	9.81E-04	3	Response to jasmonic acid stimulus
GO:0006996	1.20	2.20E-03	7	Organelle organization
GO:0008652	2.02	2.50E-03	3	Cellular amino acid biosynthetic process
GO:0033205	3.48	2.70E-03	1	Cytokinesis during cell cycle
GO:0006268	4.36	2.80E-03	1	DNA unwinding during replication
GO:0033554	1.38	4.00E-03	5	Cellular response to stress
GO:0016043	0.93	4.20E-03	10	Cellular component organization
GO:0042762	4.25	4.50E-03	1	Regulation of sulfur metabolic process
GO:0008283	2.64	4.80E-03	2	Cell proliferation
GO:0042180	1.09	1.00E-02	7	Cellular ketone metabolic process
GO:0051716	1.02	1.00E-02	8	Cellular response to stimulus
GO:0046283	3.30	1.00E-02	1	Anthocyanin metabolic process
GO:0006109	4.14	1.00E-02	1	Regulation of carbohydrate metabolic process
GO:0044106	1.40	1.00E-02	4	Cellular amine metabolic process
GO:0034641	1.16	1.00E-02	6	Cellular nitrogen compound metabolic process
GO:0042221	0.58	1.00E-02	18	Response to chemical stimulus
GO:0051726	2.20	1.00E-02	2	Regulation of cell cycle
GO:0009308	1.14	2.00E-02	6	Amine metabolic process
GO:0006520	1.42	2.00E-02	4	Cellular amino acid metabolic process
GO:0019752	1.03	2.00E-02	7	Carboxylic acid metabolic process
GO:0043436	1.03	2.00E-02	7	Oxoacid metabolic process
GO:0032392	3.86	2.00E-02	1	DNA geometric change
GO:0032508	3.86	2.00E-02	1	DNA duplex unwinding
GO:0006082	1.03	2.00E-02	7	Organic acid metabolic process
GO:0009628	0.69	3.00E-02	13	Response to abiotic stimulus
GO:0000910	2.72	3.00E-02	1	Cytokinesis
GO:0007018	2.49	3.00E-02	2	Microtubule-based movement
GO:0007017	2.06	3.00E-02	2	Microtubule-based process
GO:0009411	1.76	4.00E-02	3	Response to UV
GO:0019419	5.21	4.00E-02	1	Sulfate reduction
GO:0051276	1.60	5.00E-02	3	Chromosome organization

Down-regulated specifically in *hub1-4*

GO:0050896	0.96	2.40E-30	37	Response to stimulus
GO:0006950	1.20	5.99E-29	26	Response to stress
GO:0042221	1.13	3.33E-25	26	Response to chemical stimulus
GO:0019748	2.12	2.47E-23	9	Secondary metabolic process
GO:0006970	1.85	3.67E-22	11	Response to osmotic stress
GO:0009651	1.86	7.93E-21	10	Response to salt stress
GO:0010035	1.82	3.71E-20	10	Response to inorganic substance
GO:0016137	2.88	9.30E-20	5	Glycoside metabolic process
GO:0010038	1.86	4.49E-18	9	Response to metal ion
GO:0016143	3.13	1.15E-17	4	*S*-glycoside metabolic process
GO:0019757	3.13	1.15E-17	4	Glycosinolate metabolic process
GO:0019760	3.13	1.15E-17	4	Glucosinolate metabolic process
GO:0006952	1.59	1.36E-17	11	Defense response
GO:0005975	1.48	1.64E-17	13	Carbohydrate metabolic process
GO:0009628	1.17	6.67E-17	18	Response to abiotic stimulus
GO:0009607	1.49	1.24E-16	12	Response to biotic stimulus
GO:0051707	1.49	2.36E-16	12	Response to other organism
GO:0006790	2.45	3.19E-16	5	Sulfur metabolic process
GO:0009611	2.36	9.08E-15	5	Response to wounding
GO:0051704	1.30	4.60E-14	13	Multi-organism process
GO:0044283	1.59	8.36E-14	9	Small molecule biosynthetic process
GO:0008152	0.41	5.47E-13	56	Metabolic process
GO:0044262	1.67	1.10E-12	8	Cellular carbohydrate metabolic process
GO:0009605	1.73	7.82E-12	7	Response to external stimulus
GO:0009753	2.29	1.06E-11	4	Response to jasmonic acid stimulus
GO:0009266	1.58	2.51E-11	8	Response to temperature stimulus
GO:0010043	2.70	3.23E-11	3	Response to zinc ion
GO:0006030	2.31	9.64E-11	4	Chitin metabolic process
GO:0006022	2.29	1.39E-10	4	Aminoglycan metabolic process

GO:0044036	2.18	4.61E-10	4	Cell wall macromolecule metabolic process
GO:0009409	1.67	5.73E-10	6	Response to cold
GO:0044281	1.04	5.85E-10	14	Small molecule metabolic process
GO:0046686	1.68	7.44E-10	6	Response to cadmium ion
GO:0006037	2.33	8.66E-10	4	Cell wall chitin metabolic process
GO:0071555	2.33	8.66E-10	4	Cell wall organization
GO:0010383	2.25	1.73E-09	4	Cell wall polysaccharide metabolic process
GO:0016138	2.72	2.24E-08	3	Glycoside biosynthetic process
GO:0055114	1.19	2.30E-08	10	Oxidation reduction
GO:0016144	3.13	2.68E-08	2	S-glycoside biosynthetic process
GO:0019758	3.13	2.68E-08	2	Glycosinolate biosynthetic process
GO:0019761	3.13	2.68E-08	2	Glucosinolate biosynthetic process
GO:0005976	1.77	2.96E-08	5	Polysaccharide metabolic process
GO:0010033	0.91	3.74E-08	14	Response to organic substance
GO:0044272	2.52	3.87E-08	3	Sulfur compound biosynthetic process
GO:0006629	1.31	4.34E-08	8	Lipid metabolic process
GO:0071554	1.87	8.57E-08	4	Cell wall organization or biogenesis
GO:0009308	1.38	1.12E-07	7	Amine metabolic process
GO:0016053	1.62	2.00E-07	5	Organic acid biosynthetic process
GO:0046394	1.62	2.00E-07	5	Carboxylic acid biosynthetic process
GO:0016145	3.21	2.16E-07	2	*S*-glycoside catabolic process
GO:0019759	3.21	2.16E-07	2	Glycosinolate catabolic process
GO:0019762	3.21	2.16E-07	2	Glucosinolate catabolic process
GO:0016139	2.94	2.24E-07	2	Glycoside catabolic process
GO:0009058	0.53	2.84E-07	30	Biosynthetic process
GO:0044238	0.37	3.22E-07	46	Primary metabolic process
GO:0009414	1.67	6.66E-07	5	Response to water deprivation
GO:0044273	3.08	7.88E-07	2	Sulfur compound catabolic process
GO:0080028	3.39	8.63E-07	2	Nitrile biosynthetic process
GO:0042398	1.93	8.77E-07	4	Cellular amino acid derivative biosynthetic process
GO:0019438	1.86	1.21E-06	4	Aromatic compound biosynthetic process
GO:0009415	1.63	1.29E-06	5	Response to water
GO:0050898	3.32	1.61E-06	2	Nitrile metabolic process
GO:0080027	3.32	1.61E-06	2	Response to herbivore
GO:0044249	0.51	1.89E-06	29	Cellular biosynthetic process
GO:0006575	1.68	2.49E-06	4	Cellular amino acid derivative metabolic process
GO:0050832	1.93	2.90E-06	3	Defense response to fungus
GO:0016051	1.72	4.12E-06	4	Carbohydrate biosynthetic process
GO:0006519	1.30	4.79E-06	6	Cellular amino acid and derivative metabolic process
GO:0009699	2.14	6.73E-06	3	Phenylpropanoid biosynthetic process
GO:0034637	1.82	8.96E-06	4	Cellular carbohydrate biosynthetic process
GO:0019752	1.15	1.21E-05	7	Carboxylic acid metabolic process
GO:0043436	1.15	1.21E-05	7	Oxoacid metabolic process
GO:0006082	1.14	1.31E-05	7	Organic acid metabolic process
GO:0016052	1.82	1.51E-05	3	Carbohydrate catabolic process
GO:0009698	1.94	1.90E-05	3	Phenylpropanoid metabolic process
GO:0042180	1.13	1.96E-05	7	Cellular ketone metabolic process
GO:0006631	1.83	2.36E-05	3	Fatty acid metabolic process
GO:0044271	1.49	2.56E-05	5	Cellular nitrogen compound biosynthetic process
GO:0006725	1.45	3.46E-05	5	Cellular aromatic compound metabolic process
GO:0033037	3.32	3.87E-05	1	Polysaccharide localization
GO:0051716	1.04	3.88E-05	8	Cellular response to stimulus
GO:0009719	0.91	3.96E-05	10	Response to endogenous stimulus
GO:0042742	1.60	4.78E-05	4	Defense response to bacterium
GO:0009987	0.26	5.97E-05	54	Cellular process
GO:0006979	1.50	8.26E-05	4	Response to oxidative stress
GO:0032787	1.40	1.19E-04	5	Monocarboxylic acid metabolic process
GO:0052543	3.39	1.20E-04	1	Callose deposition in cell wall
GO:0052386	3.34	1.64E-04	1	Cell wall thickening
GO:0009620	1.42	1.89E-04	4	Response to fungus
GO:0044275	1.81	2.11E-04	3	Cellular carbohydrate catabolic process
GO:0007155	2.74	2.13E-04	2	Cell adhesion
GO:0022610	2.74	2.13E-04	2	Biological adhesion
GO:0052545	3.30	2.21E-04	1	Callose localization
GO:0009664	2.46	2.45E-04	2	Plant-type cell wall organization
GO:0006633	1.96	4.90E-04	2	Fatty acid biosynthetic process
GO:0009269	3.17	5.11E-04	1	Response to desiccation
GO:0034641	1.10	9.25E-04	6	Cellular nitrogen compound metabolic process
GO:0042430	2.48	1.50E-03	2	Indole and derivative metabolic process
GO:0042434	2.48	1.50E-03	2	Indole derivative metabolic process

GO:0071669	1.96	1.90E-03	2	Plant-type cell wall organization or biogenesis
GO:0006807	0.47	2.20E-03	21	Nitrogen compound metabolic process
GO:0044255	1.19	2.50E-03	5	Cellular lipid metabolic process
GO:0042435	2.52	3.20E-03	1	Indole derivative biosynthetic process
GO:0009908	1.31	3.20E-03	4	Flower development
GO:0052482	3.23	1.00E-02	1	Cell wall thickening during defense response
GO:0052544	3.23	1.00E-02	1	Callose deposition in cell wall during defense response
GO:0042343	3.54	1.00E-02	1	Indole glucosinolate metabolic process
GO:0010143	3.99	1.00E-02	1	Cutin biosynthetic process
GO:0007275	0.54	1.00E-02	15	Multicellular organismal development
GO:0005985	2.88	1.00E-02	1	Sucrose metabolic process
GO:0052542	3.13	1.00E-02	1	Callose deposition during defense response
GO:0031668	1.73	2.00E-02	2	Cellular response to extracellular stimulus
GO:0071496	1.73	2.00E-02	2	Cellular response to external stimulus
GO:0009759	3.86	2.00E-02	1	Indole glucosinolate biosynthetic process
GO:0080119	3.86	2.00E-02	1	ER body organization
GO:0009684	3.39	2.00E-02	1	Indoleacetic acid biosynthetic process
GO:0044237	0.25	2.00E-02	40	Cellular metabolic process
GO:0033554	1.12	2.00E-02	4	Cellular response to stress
GO:0032501	0.51	2.00E-02	15	Multicellular organismal process
GO:0009408	1.68	2.00E-02	2	Response to heat
GO:0009683	3.32	2.00E-02	1	Indoleacetic acid metabolic process
GO:0032502	0.50	3.00E-02	15	Developmental process
GO:0031669	1.80	3.00E-02	2	Cellular response to nutrient levels
GO:0009751	1.60	3.00E-02	2	Response to salicylic acid stimulus
GO:0042545	1.77	4.00E-02	2	Cell wall modification
GO:0009991	1.61	4.00E-02	2	Response to extracellular stimulus
GO:0006869	1.73	5.00E-02	2	Lipid transport

Down-regulated specifically in *khd1-1*

GO:0006259	2.56	2.35E-17	9	Cellular DNA metabolic process
GO:0006139	1.15	6.27E-16	27	Cellular nucleobase, nucleoside, nucleotide, and nucleic acid metabolic process
GO:0006807	0.90	1.11E-10	28	Nitrogen compound metabolic process
GO:0006260	3.06	3.86E-10	4	Cellular DNA replication
GO:0022402	2.46	5.21E-06	4	Cell cycle process
GO:0007049	2.01	6.90E-05	4	Cell cycle
GO:0048367	1.89	6.92E-05	5	Shoot development
GO:0022621	1.87	9.28E-05	5	Shoot system development
GO:0044260	0.49	9.93E-05	36	Cellular macromolecule metabolic process
GO:0006261	3.18	1.37E-04	2	DNA-dependent DNA replication
GO:0048827	2.05	1.90E-04	4	Phyllome development
GO:0043170	0.44	3.85E-04	39	Macromolecule metabolic process
GO:0006281	2.13	7.89E-04	3	DNA repair
GO:0034984	2.13	8.39E-04	3	Cellular response to DNA damage stimulus
GO:0009987	0.30	1.20E-03	55	Cellular process
GO:0016070	0.93	1.30E-03	12	Cellular RNA metabolic process
GO:0006974	2.07	1.40E-03	3	Response to DNA damage stimulus
GO:0022403	2.48	1.50E-03	3	Cell cycle phase
GO:0031323	0.84	1.70E-03	14	Regulation of cellular metabolic process
GO:0044237	0.37	1.90E-03	44	Cellular metabolic process
GO:0051171	0.85	2.80E-03	13	Regulation of nitrogen compound metabolic process
GO:0019219	0.84	3.80E-03	13	Regulation of cellular nucleobase, nucleoside, nucleotide, and nucleic acid metabolic process
GO:0009887	2.03	4.20E-03	3	Organ morphogenesis
GO:0044238	0.34	4.30E-03	45	Primary metabolic process
GO:0019222	0.75	1.00E-02	15	Regulation of metabolic process
GO:0031326	0.80	1.00E-02	13	Regulation of cellular biosynthetic process
GO:0009889	0.80	1.00E-02	13	Regulation of biosynthetic process
GO:0006350	0.79	1.00E-02	13	Cellular transcription
GO:0061018	0.79	1.00E-02	13	Transcription
GO:0008152	0.28	1.00E-02	51	Metabolic process
GO:0010467	0.56	1.00E-02	21	Gene expression
GO:0080090	0.77	1.00E-02	13	Regulation of primary metabolic process
GO:0048608	0.95	1.00E-02	9	Reproductive structure development
GO:0007126	2.83	1.00E-02	2	Meiosis
GO:0051327	2.83	1.00E-02	2	M phase of meiotic cell cycle
GO:0000279	2.43	2.00E-02	2	M phase
GO:0045449	0.79	2.00E-02	12	Regulation of cellular transcription
GO:0061019	0.79	2.00E-02	12	Regulation of transcription
GO:0010556	0.78	2.00E-02	12	Regulation of macromolecule biosynthetic process

GO:0048366	1.83	2.00E-02	3	Leaf development
GO:0022414	0.85	2.00E-02	11	Reproductive process
GO:0010468	0.74	2.00E-02	13	Regulation of gene expression
GO:0060255	0.73	2.00E-02	14	Regulation of macromolecule metabolic process
GO:0009451	2.20	3.00E-02	2	RNA modification
GO:0032501	0.64	3.00E-02	16	Multicellular organismal process
GO:0000003	0.83	3.00E-02	11	Reproduction
GO:0007275	0.64	3.00E-02	16	Multicellular organismal development
GO:0007017	2.16	3.00E-02	2	Microtubule-based process
GO:0042254	1.84	3.00E-02	3	Ribosome biogenesis
GO:0009888	1.49	4.00E-02	4	Tissue development
GO:0003006	0.86	5.00E-02	9	Reproductive developmental process

Down-regulated specifically in *spen3-1*

GO:0023046	1.18	3.00E-02	10	Signaling process
GO:0023060	1.18	3.00E-02	10	Signal transmission
GO:0007623	2.80	5.00E-02	3	Circadian rhythm
GO:0048511	2.80	5.00E-02	3	Rhythmic process

Up-regulated in *hub1-4* and *khd1-1*

GO:0050896	1.15	1.09E-25	42	Response to stimulus
GO:0009725	2.00	1.78E-24	20	Response to hormone stimulus
GO:0010033	1.67	7.16E-24	25	Response to organic substance
GO:0009719	1.91	8.64E-24	20	Response to endogenous stimulus
GO:0009733	2.76	2.17E-23	12	Response to auxin stimulus
GO:0042221	1.27	9.13E-18	28	Response to chemical stimulus
GO:0009741	3.53	2.69E-09	4	Response to brassinosteroid stimulus
GO:0023052	1.26	9.32E-08	15	Signaling
GO:0032870	2.25	1.09E-07	6	Cellular response to hormone stimulus
GO:0007165	1.43	1.25E-07	12	Signal transduction
GO:0009755	2.24	3.00E-07	6	Hormone-mediated signaling pathway
GO:0051704	1.32	4.12E-07	13	Multi-organism process
GO:0009607	1.42	4.20E-07	11	Response to biotic stimulus
GO:0023046	1.38	4.87E-07	12	Signaling process
GO:0023060	1.38	4.87E-07	12	Signal transmission
GO:0051707	1.43	5.50E-07	11	Response to other organism
GO:0071495	2.10	1.00E-06	6	Cellular response to endogenous stimulus
GO:0007242	1.61	1.34E-06	9	Intracellular signaling cascade
GO:0051716	1.43	1.97E-06	10	Cellular response to stimulus
GO:0006952	1.44	2.24E-06	10	Defense response
GO:0065008	1.51	3.19E-06	9	Regulation of biological quality
GO:0009606	3.47	3.45E-06	3	Tropism
GO:0006468	1.39	5.67E-06	10	Protein amino acid phosphorylation
GO:0065007	0.72	8.30E-06	27	Biological regulation
GO:0006796	1.25	1.70E-05	11	Phosphate metabolic process
GO:0006793	1.24	1.78E-05	11	Phosphorus metabolic process
GO:0071310	1.83	2.12E-05	6	Cellular response to organic substance
GO:0055085	1.59	4.24E-05	7	Transmembrane transport
GO:0006464	1.00	4.57E-05	15	Protein modification process
GO:0043687	1.12	4.94E-05	13	Post-translational protein modification
GO:0016310	1.24	7.49E-05	10	Phosphorylation
GO:0006950	0.80	1.07E-04	20	Response to stress
GO:0009630	3.39	1.44E-04	2	Gravitropism
GO:0070887	1.66	2.05E-04	6	Cellular response to chemical stimulus
GO:0008219	1.90	4.16E-04	5	Cell death
GO:0016265	1.90	4.16E-04	5	Death
GO:0016049	1.83	4.56E-04	5	Cell growth
GO:0009639	2.17	4.97E-04	4	Response to red or far red light
GO:0009629	3.18	5.31E-04	2	Response to gravity
GO:0043412	0.89	6.22E-04	15	Macromolecule modification
GO:0012501	1.97	7.42E-04	4	Programmed cell death
GO:0008361	1.76	9.31E-04	5	Regulation of cell size
GO:0032535	1.74	1.20E-03	5	Regulation of cellular component size
GO:0090066	1.74	1.20E-03	5	Regulation of anatomical structure size
GO:0051179	0.90	1.40E-03	14	Localization
GO:0040007	1.61	1.70E-03	5	Growth
GO:0048589	1.81	1.80E-03	5	Developmental growth
GO:0006810	0.90	1.90E-03	14	Transport
GO:0009638	4.44	1.90E-03	1	Phototropism
GO:0051234	0.90	2.10E-03	14	Establishment of localization

GO:0050789	0.63	2.40E-03	23	Regulation of biological process
GO:0009605	1.49	2.60E-03	6	Response to external stimulus
GO:0080086	5.03	3.20E-03	1	Stamen filament development
GO:0009692	3.76	3.80E-03	1	Ethylene metabolic process
GO:0009693	3.76	3.80E-03	1	Ethylene biosynthetic process
GO:0043449	3.71	4.70E-03	1	Cellular alkene metabolic process
GO:0043450	3.71	4.70E-03	1	Alkene biosynthetic process
GO:0050832	1.99	1.00E-02	4	Defense response to fungus
GO:0050794	0.64	1.00E-02	20	Regulation of cellular process
GO:0042742	1.71	1.00E-02	4	Defense response to bacterium
GO:0009742	3.16	1.00E-02	2	Brassinosteroid mediated signaling pathway
GO:0043401	3.16	1.00E-02	2	Steroid hormone mediated signaling pathway
GO:0048545	3.16	1.00E-02	2	Response to steroid hormone stimulus
GO:0071367	3.16	1.00E-02	2	Cellular response to brassinosteroid stimulus
GO:0071383	3.16	1.00E-02	2	Cellular response to steroid hormone stimulus
GO:0044042	2.26	2.00E-02	3	Glucan metabolic process
GO:0010359	4.44	2.00E-02	1	Regulation of anion channel activity
GO:0022898	4.44	2.00E-02	1	Regulation of transmembrane transporter activity
GO:0032409	4.44	2.00E-02	1	Regulation of transporter activity
GO:0032412	4.44	2.00E-02	1	Regulation of ion transmembrane transporter activity
GO:0034762	4.44	2.00E-02	1	Regulation of transmembrane transport
GO:0034765	4.44	2.00E-02	1	Regulation of ion transmembrane transport
GO:0044070	4.44	2.00E-02	1	Regulation of anion transport
GO:0009416	1.21	2.00E-02	7	Response to light stimulus
GO:0000902	1.66	2.00E-02	4	Cell morphogenesis
GO:0009314	1.18	3.00E-02	7	Response to radiation
GO:0005976	1.55	3.00E-02	4	Polysaccharide metabolic process
GO:0010200	1.72	4.00E-02	4	Response to chitin

Up-regulated in *hub1-4* and *spen3-1*

GO:0050896	1.39	2.17E-08	50	Response to stimulus
GO:0042221	1.49	4.43E-05	33	Response to chemical stimulus
GO:0006952	2.27	6.45E-05	18	Defense response
GO:0010033	1.64	8.04E-04	24	Response to organic substance
GO:0051704	1.90	8.14E-04	19	Multi-organism process
GO:0051707	2.03	1.20E-03	17	Response to other organism
GO:0009607	2.00	1.60E-03	17	Response to biotic stimulus
GO:0065008	2.18	2.00E-03	15	Regulation of biological quality
GO:0012501	3.05	2.30E-03	9	Programmed cell death
GO:0006950	1.31	3.70E-03	28	Response to stress
GO:0009626	4.13	4.50E-03	6	Plant-type hypersensitive response
GO:0042592	2.92	4.60E-03	9	Homeostatic process
GO:0034050	4.11	4.70E-03	6	Host programmed cell death induced by symbiont
GO:0009719	1.76	1.00E-02	18	Response to endogenous stimulus
GO:0008219	2.83	1.00E-02	9	Cell death
GO:0016265	2.83	1.00E-02	9	Death
GO:0009987	0.52	4.00E-02	65	Cellular process

Up-regulated specifically in *hub1-4*

GO:0050896	0.82	3.06E-11	34	Response to stimulus
GO:0006950	0.69	2.10E-03	19	Response to stress
GO:0065007	0.56	3.30E-03	25	Biological regulation
GO:0007623	2.53	1.00E-02	2	Circadian rhythm
GO:0048511	2.53	1.00E-02	2	Rhythmic process
GO:0009987	0.27	1.00E-02	55	Cellular process
GO:0023052	0.86	1.00E-02	11	Signaling
GO:0016310	1.00	1.00E-02	9	Phosphorylation
GO:0000160	2.43	2.00E-02	2	Two-component signal transduction system (phosphorelay)
GO:0006796	0.94	2.00E-02	9	Phosphate metabolic process
GO:0006793	0.94	2.00E-02	9	Phosphorus metabolic process
GO:0006468	1.03	2.00E-02	8	Protein amino acid phosphorylation
GO:0044237	0.32	3.00E-02	42	Cellular metabolic process

Up-regulated specifically in *khd1-1*

GO:0050896	1.1	3.53E-19	41	Response to stimulus
GO:0042221	1.23	1.19E-13	28	Response to chemical stimulus
GO:0006950	1.19	4.49E-12	26	Response to stress
GO:0010033	1.21	1.28E-07	18	Response to organic substance
GO:0006979	2.11	4.37E-06	6	Response to oxidative stress
GO:0006952	1.41	7.54E-05	10	Defense response

GO:0065007	0.71	1.15E-04	27	Biological regulation
GO:0009741	3.17	1.55E-04	3	Response to brassinosteroid stimulus
GO:0040007	1.77	4.93E-04	6	Growth
GO:0009607	1.27	5.13E-04	10	Response to biotic stimulus
GO:0009628	0.97	6.55E-04	15	Response to abiotic stimulus
GO:0051707	1.27	7.53E-04	10	Response to other organism
GO:0051704	1.14	1.10E-03	11	Multi-organism process
GO:0009651	1.45	1.20E-03	8	Response to salt stress
GO:0006970	1.41	1.30E-03	8	Response to osmotic stress
GO:0065008	1.36	1.70E-03	8	Regulation of biological quality
GO:0009719	1.09	2.80E-03	11	Response to endogenous stimulus
GO:0016049	1.83	3.00E-03	5	Cell growth
GO:0050832	2.11	4.30E-03	4	Defense response to fungus
GO:0009725	1.11	4.30E-03	11	Response to hormone stimulus
GO:0008361	1.77	1.00E-02	5	Regulation of cell size
GO:0006869	2.41	1.00E-02	3	Lipid transport
GO:0032535	1.75	1.00E-02	5	Regulation of cellular component size
GO:0090066	1.75	1.00E-02	5	Regulation of anatomical structure size
GO:0019748	1.52	1.00E-02	6	Secondary metabolic process
GO:0050789	0.63	1.00E-02	23	Regulation of biological process
GO:0023052	0.96	1.00E-02	12	Signaling
GO:0010876	2.25	2.00E-02	3	Lipid localization
GO:0032502	0.72	2.00E-02	18	Developmental process
GO:0050794	0.65	2.00E-02	21	Regulation of cellular process
GO:0055114	1.09	3.00E-02	9	Oxidation reduction
GO:0006810	0.85	3.00E-02	13	Transport
GO:0051234	0.84	4.00E-02	13	Establishment of localization
Up-regulated specifically in *spen3-1*				
GO:0050896	0.79	3.05E-05	33	Response to stimulus
GO:0042221	1.01	3.68E-05	24	Response to chemical stimulus
GO:0009607	1.42	8.29E-04	11	Response to biotic stimulus
GO:0051707	1.40	0.0015	11	Response to other organism
GO:0008152	0.40	0.0037	56	Metabolic process
GO:0009628	1.01	0.01	16	Response to abiotic stimulus
GO:0051704	1.19	0.01	12	Multi-organism process
GO:0055114	1.29	0.01	10	Oxidation reduction
GO:0042542	3.43	0.01	2	Response to hydrogen peroxide
GO:0015893	3.05	0.02	3	Drug transport
GO:0042493	3.04	0.02	3	Response to drug
GO:0006979	1.89	0.02	6	Response to oxidative stress
GO:0000302	2.96	0.02	3	Response to reactive oxygen species
GO:0010035	1.43	0.03	8	Response to inorganic substance

Table S3. Primer sequences

Gene	AGI code	Primer set	Forward Primer Sequence	Reverse Primer Sequence
Real-time qPCR				
SPEN3	At1g27750		CCCTGCATCAAGTCCCATGT	ACCGATCAAGCATTCCGAGG
KHD1	At1g51580		CCCCATTTGGACCGAGACAA	CCAGGACCATGACAATGCCT
CCA1	At2g46830		CCATGGAAGCCAAAGAAAGT	GGAAGCTTGAGTTTCCAACC
PP2A	At1g13320		TAACGTGGCCAAAATGATGC	GTTCTCCACAACCGCTTGGT
UBC	At5g25760		CTGCGACTCAGGGAATCTTCTAA	TTGTGCCATTGAATTGAACCC
FLC	At5g10140		CCTCTCCGTGACTAGAGCCAAG	AGGTGACATCTCCATCTCAGCTTC
FLC2			TTTGTCCAGCAGGTGACATC	AGCCAAGAAGACCGAACTCA
totalCOOLAIR			GCCGTAGGCTTCTTCACTGT	TGTATGTGTTCTTCACTTCTGTCAA
proxCOOLAIR			CACACCACCAAATAACAACCA	TTTTTTTTTTTTTTTACTGCTTCCA
distCOOLAIR			GGGGTAAACGAGAGTGATGC	TTTTTTTTTTTTTTTGCGGTACAC
CCA1α			GATCTGGTTATTAAGACTCGGAAGCCATATAC	GCCTCTTTCTCTACCTTGGAGA
CCA1β			GAATGTTCCTTGTGATAAGCCATAGAGG	AGGATCGTTCCACTTCCCGTCTT
	At1g77920		CGAGTCCACGCATTATCCCA	CCTCGAGCCGATTGTCTTGT
	At1g77930		TCGAGCTTGATACCGAAGCAG	AGAGACAGAGAGGGAGCAAGT
ChIP-qPCR				
CCA1	At2g46830	P1	GAACAAGTTGATGTTAAGATGGAC	GGAGAAATCTCAGCCACTATAATTATC
		P2	GAAGTTGTGTAGAGGAGCTTAGTG	CTTCCTCAGTCCACCTTTCACGTTGC
		P3	ATCCTCGAAAGACGGGAAGT	GTCGATCTTCATTGGCCATC
		P4	AAGGCTCGATCTTCACTGGA	CCATCCTCTTGCCTTTCTGA
		P5	CTCAAGCTTCCACATGAGACTC	GTTACAGGAAGACTATGGACAAG
FLC	At5g10140	P1	GTTCGGGAGATTAACACAAATAATAAAGG	GAAAACAAGCTGATACAAGCATTTCAC
		P2	GCTGGACCTAACTAGGGGTGAAC	CCTCTTTGGTACGGATCTATAATGAATC
		P3	CCTCTCCGTGACTAGAGCCAAG	CTTCAACATGAGTTCGGTCTGC
		P4	CCTTGGATAGAAGACAAAAAGAGAAAGTG	AGGTGACATCTCCATCTCAGCTTC
Cloning				
KHD1N			ACAGGATCCAAACGTCCGGCGACGACA	ACAGTCGACTCAACTCGTCCCATGTTGGA
RRMSPEN3			CACGGATCCACTCTACGGATCGTAGGAA	CACGTCGACTCAAATCCTTTCACTGGATCAAA
EMSA				
RNA			AAAACAAAAUAGCACCGUAAAGCAC	
DNA			AAAACAAAATACCAGCGTAAAGCAC	

Supplemental dataset S1 (separate file)

Protein Identification details obtained with the 4800 MALDI TOF/TOFTM Proteomics analyzer (AB SCIEX) and the GPS explorer v3.6 (AB SCIEX) software package combined with the search engine Mascot version 2.1 (Matrix Science) and database TAIR8.

Supporting references

1. Alonso JM, et al. (2003) Genome-wide insertional mutagenesis of *Arabidopsis thaliana*. *Science* 301(5633), 653-657 [Err. *Science* 301(5641), 1849].
2. Rosso MG, et al. (2003) An *Arabidopsis thaliana* T-DNA mutagenized population (GABI-Kat) for flanking sequence tag-based reverse genetics. *Plant Mol Biol* 53(1-2), 247-259.
3. Sessions A, et al. (2002) A high-throughput Arabidopsis reverse genetics system. *Plant Cell* 14(12), 2985-2994.
4. Fleury D, et al. (2007) The *Arabidopsis thaliana* homolog of yeast *BRE1* has a function in cell cycle regulation during early leaf and root growth. *Plant Cell* 19(2), 417-432.
5. Salomé PA, McClung R (2005) *PSEUDO-RESPONSE REGULATOR7* and *9* are partially redundant genes essential for the temperature responsiveness of the Arabidopsis circadian clock. *Plant Cell* 17(3), 791-803.
6. Portolés S, Más P (2007) Altered oscillator function affects clock resonance and is responsible for the reduced day-length sensitivity of CKB4 overexpressing plants. *Plant J* 51(6), 966-977.
7. Dhondt S, et al. (2014) High-resolution time-resolved imaging of *in vitro* Arabidopsis rosette growth. *Plant J* 80(1), 172-184.
8. Skirycz A, et al. (2011) Survival and growth of *Arabidopsis* plants given limited water are not equal. *Nat. Biotechnol* 29(3), 212-214.
9. Clauw P, et al. (2015) Leaf responses to mild drought stress in natural variants of Arabidopsis. *Plant Physiol* 167(3), 800-816. [Corrigendum Plant Physiol. 168(3), 1180].
10. Coppens F, Wuyts N, Inzé D, Dhondt S (2017) Unlocking the potential of plant phenotyping data through integration and data-driven approaches. *Curr Opin Syst Biol* 4, 58-63.
11. Moore A, Zielinski T, Millar AJ (2014) Online period estimation and determination of rhythmicity in circadian data, using the BioDare data infrastructure. *Methods Mol Biol* 1158, 13-44.
12. Van Bel M, et al. (2012) Dissecting plant genomes with the PLAZA comparative genomics platform. *Plant Physiol* 158(2), 590-600.
13. Bruno L, et al. (2011) Multi-probe *in situ* hybridization to whole mount *Arabidopsis* seedlings. *Int J Dev Biol* 55 (2), 197-203.
14. Casamitjana-Martínez E, et al. (2003) Root-specific *CLE19* overexpression and the *sol1/2* suppressors implicate a CLV-like pathway in the control of *Arabidopsis* root meristem maintenance. *Curr Biol* 13(16), 1435-1441.
15. Rigaut G, et al. (1999) A generic protein purification method for protein complex characterization and proteome exploration. *Nat Biotechnol* 17(10), 1030-1032.
16. Bürckstümmer T, et al. (2006) An efficient tandem affinity purification procedure for interaction proteomics in mammalian cells. *Nat Methods* 3(12), 1013-1019.
17. Van Leene J, et al. (2007) A tandem affinity purification-based technology platform to study the cell cycle interactome in *Arabidopsis thaliana*. *Mol Cell Proteomics* 6(7), 1226-1238.
18. Van Leene J, et al. (2010) Targeted interactomics reveals a complex core cell cycle machinery in *Arabidopsis thaliana*. *Mol Syst Biol* 6(1), 397.
19. Krohn NM, Yanagisawa S, Grasser KD (2002) Specificity of the stimulatory interaction between chromosomal HMGB proteins and the transcription factor Dof2 and its negative regulation by protein kinase CK2-mediated phosphorylation. *J Biol Chem* 277(36), 32438-32444.
20. Kammel C, et al. (2013) *Arabidopsis* DEAD-box RNA helicase UAP56 interacts with both RNA and DNA as well as with mRNA export factors. *PLoS ONE* 8(3), e60644.

21. Shen J, Zhang L, Zhao R (2007) Biochemical characterization of the ATPase and helicase activity of UAP56, an essential pre-mRNA splicing and mRNA export factor. *J Biol Chem* 282(31), 22544-22550.
22. Cao Y, Dai Y, Cui S, Ma L (2008) Histone H2B monoubiquitination in the chromatin of *FLOWERING LOCUS C* regulates flowering time in *Arabidopsis*. *Plant Cell* 20(10), 2586-2602.
23. Guindon S, et al. (2010) New algorithms and methods to estimate maximum-likelihood phylogenies: assessing the performance of PhyML 3.0. *Syst Biol* 59(3), 307–321.
24. Guindon S, Gascuel O (2003) A simple, fast, and accurate algorithm to estimate large phylogenies by maximum likelihood. *Syst Biol* 52(5), 696-704.
25. Ronquist F, et al. (2012) MrBayes 3.2: efficient Bayesian phylogenetic inference and model choice across a large model space. *Syst Biol* 61(3), 539-542.
26. Kumar S, Stecher G, Li M, Knyaz C, Tamura K (2018) MEGA X: Molecular Evolutionary Genetics Analysis across Computing Platforms. *Mol Biol Evol* 35(6), 1547-1549.